

Electronic Supplementary Information

**Controllable preparation of core-shell magnetic covalent-organic framework
nanospheres for efficient adsorption and removal of bisphenols in aqueous
solution**

Yang Li, Cheng-Xiong Yang*, and Xiu-Ping Yan*

Materials and Reagents. All chemicals and reagents used are at least of analytical grade. Ultrapure water was purchased from Wahaha Foods Co. (Tianjin, China). 1,3,5-Triformylphloroglucinol (Tp) was obtained from Chengdu Tongchuangyuan Pharmaceutical Technology Co. (Chengdu, China), benzidine (BD), $\text{FeCl}_3 \cdot 6\text{H}_2\text{O}$, ethylene glycol (EG), poly(4-styrenesulfonic acid-co-maleic acid, SS:MA=3:1)sodium salt (PSSMA 3:1, M_w 20000), anhydrous sodium acetate, tetraethyl orthosilicate (TEOS), 3-aminopropyltriethoxysilane (APTES), bisphenol A (BPA), 4,4'-(hexafluoroisopropylidene)diphenol (BPAF), 4-cumylphenol, diphenylmethane were obtained from Aladdin Chemistry Co. (Shanghai, China). 1,4-Dioxane, mesitylene, acetic acid, ammonium hydroxide solution, methanol, ethanol, isopropanol, cyclohexane, acetonitrile, tetrahydrofuran (THF), N,N-dimethylformamide (DMF) and dichloromethane (DCM) were purchased from Concord Fine Chemical Research Institute (Tianjin, China). Toluene was purchased from Guangfu Fine Chemical Research Institute (Tianjin, China).

Instrumentation. X-ray diffraction spectrometry (XRD) patterns were recorded on a D/max-2500 diffractometer (Rigaku, Japan) with Cu $K\alpha$ radiation ($\lambda = 1.5418 \text{ \AA}$) over the angular range from 2° to 70° . The morphology of the materials was characterized on a Shimadzu SS-550 scanning electron microscope at 15.0 kV. A Magna-560 spectrometer (Nicolet, Madison, WI) was used to record the Fourier transform infrared (FT-IR) spectra in KBr plate. Zeta potentials of the adsorbent in ultrapure water were measured on a Zeta potential analyzer (Brookhaven Instruments Co., Holtsville, NY, USA). Thermogravimetric analysis (TGA) was accomplished on a PTC-10A thermal gravimetric analyzer (Rigaku, Japan) from room temperature to 700°C at a heating rate of $10^\circ\text{C min}^{-1}$. Brunauer-Emmett-Teller (BET) surface area, pore volume and pore size distribution of the materials were measured on A NOVA 2000e surface area and pore size analyzer (Quantachrome, Florida, FL, USA)

using nitrogen adsorption at 77 K in the range $0.02 \leq P/P_0 \leq 0.20$. Transmission electron microscopy (TEM) characterization was performed on Tecnai G2 F20 (Philips, Holland) at 200 kV. High angle annular dark field scanning transmission electron microscopy (HAADF-STEM) imaging and energy-dispersive X-ray spectroscopy (EDX) elemental mapping were performed on FEI Tecnai G2 F20 S-TWIN at 200 kV. The magnetic properties were studied on a LDJ 9600-1 vibrating sample magnetometer (VSM) (LDJ Electronics Inc., Troy, MI, USA) at room temperature by cycling the field from -10 to 10 kOe. The absorption spectra were recorded on a UV-3600 UV-vis-NIR spectrophotometer (Shimadzu, Japan) with 1 cm path-length cells.

Synthesis of Fe₃O₄ Magnetic Nanospheres. Magnetic Fe₃O₄ nanospheres were prepared based on a solvothermal method (J. N. Gao, X. Z. Ran, C. M. Shi, T. M. Cheng, Y. P. Su, *Nanoscale* 2013, 5, 7026). Briefly, 0.7 g PSSMA was dissolved in 10 mL EG by mechanical stirring, followed by addition of 10 mL EG solution of 0.81 g FeCl₃·6H₂O, and 1.8 g sodium acetate was put in afterwards. The obtained solution was transferred into a Teflon-lined stainless-steel autoclave and heated at 200 °C for 10 h. After cooling to room temperature, the dark product was separated by a magnet and washed with water three times, ethanol once, and then dried under vacuum for 12 h.

Synthesis of Amino Functionalized Fe₃O₄ Nanospheres (Fe₃O₄-NH₂). 150 mg Fe₃O₄ nanospheres were dispersed in 100 mL ethanol. After being ultrasonicated for 30 min, 25 mL water and 1.2 mL ammonium hydroxide solution were added under mechanical stirring, then 100 µL TEOS in 5 mL ethanol was put into the system. The reaction was allowed to proceed for 9 h. The obtained particles were collected by a magnet and washed three times with ethanol and water. The obtained product above was dispersed in 120 mL isopropanol, followed by addition of 0.5 mL APTES. After 9 h mechanically stirring, the product was isolated and washed with water and ethanol and then dried in vacuum oven overnight.

Synthesis of Tp Functionalized Fe₃O₄ Nanospheres (Fe₃O₄-Tp). Fe₃O₄-NH₂ (150 mg) was dispersed in dioxane (10 mL), followed by adding Tp (10 mg) and acetic acid (150 μL). The mixture was sonicated for 3 min, then transferred into a Teflon-lined stainless-steel autoclave and heated at 120°C for 1 h. The product was separated by a magnet and sequentially washed with DMF, dioxane and mesitylene for subsequent reaction.

Synthesis of TpBD. TpBD was synthesized under solvothermal conditions by co-condensation of Tp and BD using acetic acid as catalyst (S. Chandra, S. Kandambeth, B. P. Biswal, B. Lukose, S. M. Kunjir, M. Chaudhary, R. Babarao, T. Heine, R. Banerjee, J. Am. Chem. Soc. 2013, 135, 17853). Tp (0.3 mmol) in mesitylene/dioxane (1:1) (3 mL), BD (0.45 mmol) in mesitylene/dioxane (1:1) (3 mL) and aqueous acetic acid (0.5 mL, 9 M) were mixed. The mixture was sonicated for 3 min, then transferred into a Teflon-lined stainless-steel autoclave and heated at 120°C for 48 h. The precipitate was collected by filtration and washed with DMF thrice and DCM/acetone twice. The collected powder was dried in vacuum overnight.

In Situ Synthesis of Fe₃O₄@TpBD Core-Shell Nanospheres. Typically, the as-synthesized Fe₃O₄-Tp (50 mg) was dispersed in mesitylene/dioxane (1:1) (2.5 mL), and mixed with Tp solution in mesitylene/dioxane (1:1) (0.1 mmol, 1 mL), BD solution in mesitylene/dioxane (1:1) (0.15 mmol, 1 mL) and aqueous acetic acid (9 M, 0.5 mL). After sonication for 3 min, the mixture was transferred into a Teflon-lined stainless-steel autoclave and heated at 120 °C for 48 h. The product was isolated with the help of magnet, washed with DMF until the supernatant became clear, then washed with DCM/acetone twice before being dried under vacuum overnight.

Layer-by-layer Synthesis of Fe₃O₄@TpBD Core-Shell Nanospheres. Typically, the as-synthesized Fe₃O₄-Tp (50 mg) was dispersed in mesitylene/dioxane (1:1) (2.5 mL), then

mixed with BD(0.015 mmol) or Tp (0.01 mmol) in mesitylene/dioxane (1:1) (1 mL) and aqueous acetic acid (0.5 mL, 9 M). The mixture was sonicated for 3 min, then transferred into a Teflon-lined stainless-steel autoclave and heated at 120 °C for 1 h. At each step the product was isolated with the help of magnet, washed with DMF and dioxane. After a given number of cycles, the product was washed with DMF, THF and DCM sequentially, then dried under vacuum overnight.

Adsorption Experiments. In general, Fe₃O₄@TpBD (5 mg) was dispersed in BPA or BPAF aqueous solution (5 mL) with certain initial concentration. After adsorption at a controlled temperature for a given time, the mixture was isolated by a magnet and the supernatant was filtered with 0.22 μm Millipore cellulose membrane before UV-visible absorption spectrum analysis.

To test the effect of ionic strength, certain amounts of NaCl or MgSO₄ were included in BPA and BPAF aqueous solution. To evaluate pH effect, BPA and BPAF aqueous solutions were adjusted with diluted NaOH and HCl in a pH range from 3 to 10.

Desorption Experiments. Typically, the BPA or BPAF pre-adsorbed Fe₃O₄@TpBD was treated with ethanol (0.5 mL) under ultrasonication for 1 min. The mixture was then magnetically separated. The collected supernatant was filtered with 0.22 μm Millipore cellulose membrane before UV-vis absorption analysis. For reusability investigation, the desorbed Fe₃O₄@TpBD was washed with ethanol and dried for another adsorption cycle.

Kinetic Equations for Adsorption Study. The pseudo-first-order kinetics equation is given as follows:

$$\ln(q_e - q_t) = \ln q_e - k_1 t \quad (1)$$

where q_t and q_e are the adsorption capacity (mg g⁻¹) at a given time t (min) and at equilibrium, respectively, and k_1 is the rate constant for the pseudo-first-order adsorption

(min⁻¹).

The pseudo-second-order kinetics equation is given as follows:

$$dq_t/dt=k_2(q_e-q_t)^2 \quad (2)$$

$$t/q_t=1/(k_2q_e^2)+t/q_e \quad (3)$$

q_t is the adsorption capacity (mg g⁻¹) at given time t (min) and q_e is the adsorption capacity at equilibrium (mg g⁻¹). k_2 is the rate constant of pseudo-second-order adsorption (g mg⁻¹ min⁻¹).

Thermodynamic Equations for Adsorption Study. Freundlich model equation is given as follows:

$$q_e=K_F C_e^{1/n} \quad (4)$$

where q_e (mg g⁻¹) is the equilibrium adsorption capacity of BPA or BPAF, C_e (mg L⁻¹) is the concentration of BPA or BPAF at equilibrium, K_F [(mg g⁻¹)/(mg L⁻¹)^(1/n)] is the Freundlich affinity coefficient and n is related to surface heterogeneity.

Langmuir model equations given as follows:

$$q_e=C_e q_0 b / (C_e b + 1) \quad (5)$$

where q_e (mg g⁻¹) is the equilibrium adsorption capacity, C_e (mg L⁻¹) is the concentration of BPA or BPAF at equilibrium, q_0 (mg g⁻¹) is the maximum adsorption capacity, b (L mg⁻¹) is the Langmuir constant.

The thermodynamic parameters, enthalpy change (ΔH , kJ mol⁻¹), free energy change (ΔG , kJ mol⁻¹), entropy change (ΔS , J mol⁻¹ K⁻¹) and the thermodynamic equilibrium constant (K_0) for the adsorption behavior were determined based on the following equations:

$$K_0=q_e/C_e \quad (6)$$

$$\Delta G=-RT \ln K_0 \quad (7)$$

$$\ln K_0=\Delta S/R-\Delta H/(RT) \quad (8)$$

where q_e (mg g⁻¹) is the equilibrium adsorption capacity of BPA or BPAF, C_e (mg L⁻¹) is the

concentration of BPA or BPAF at equilibrium, R is the universal gas constant ($8.314 \text{ J mol}^{-1} \text{ K}^{-1}$). K_0 can be obtained by plotting $\ln(q_e/C_e)$ versus q_e . ΔH and ΔS were calculated from the plot of $\ln K_0$ versus $1/T$ according to equation (8).

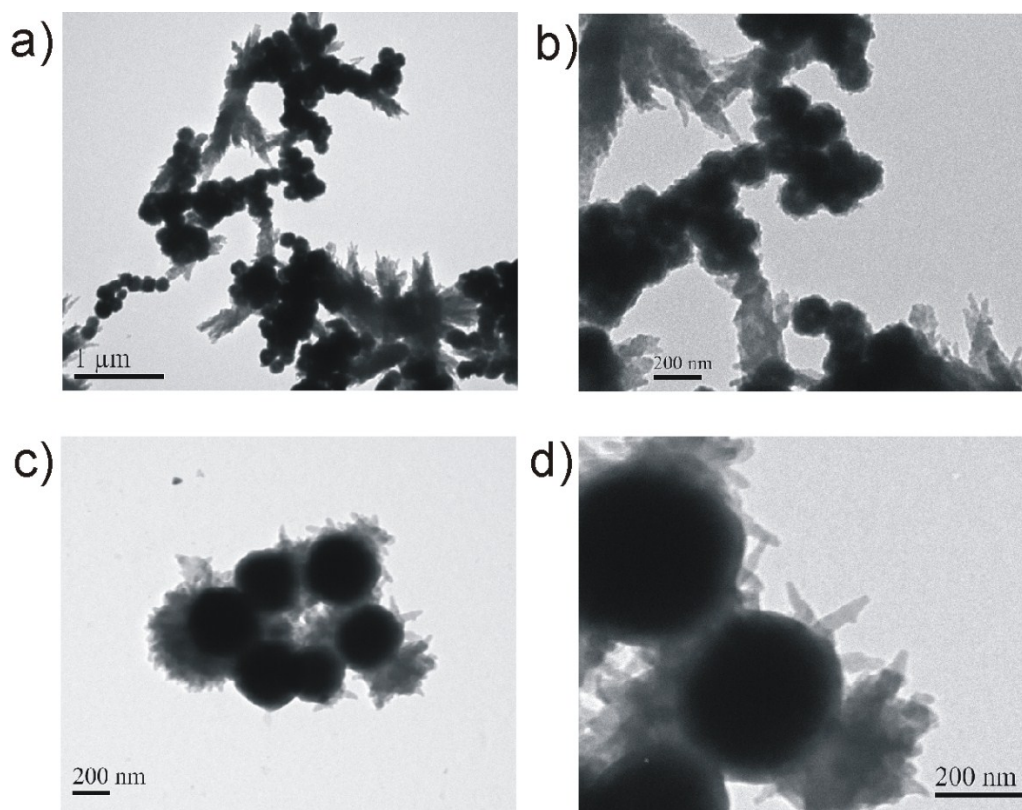


Figure S1. a,b) TEM images of Fe₃O₄-TpBD prepared by direct growth of TpBD on Fe₃O₄ without silanization reagent nor Tp coating. c,d) TEM images of Fe₃O₄-NH₂-TpBD prepared by direct growth of TpBD on Fe₃O₄-NH₂ without Tp coating.

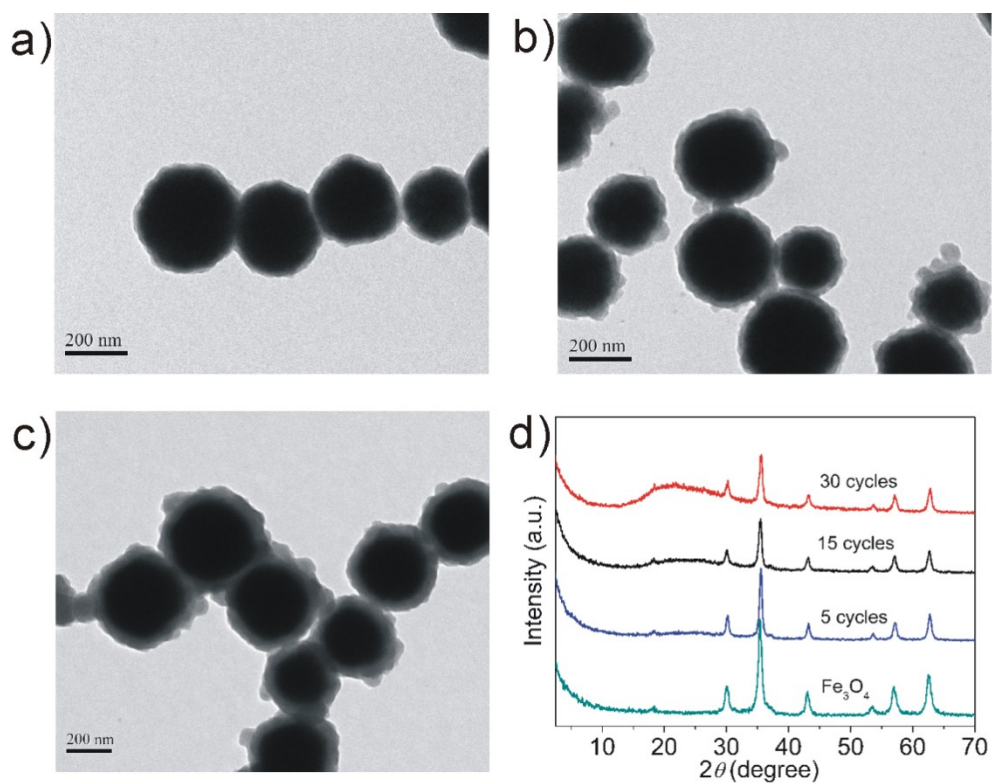


Figure S2. TEM images of the $\text{Fe}_3\text{O}_4@\text{TpBD}$ prepared by a layer-by-layer growth method: a) 5 cycles, b) 15 cycles, c) 30 cycles. d) XRD pattern of corresponding materials.

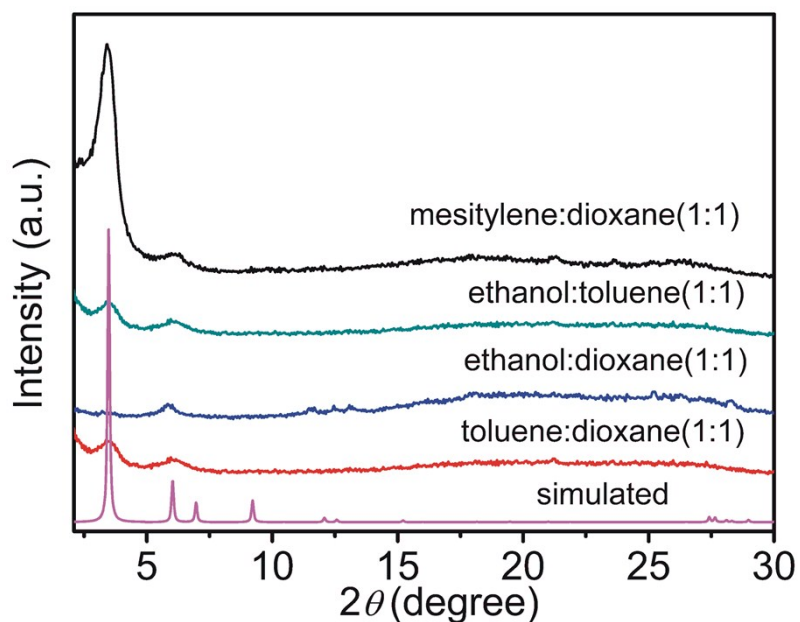


Figure S3. XRD pattern of TpBD prepared in different solvents by a monomer-mediated in situ growth strategy.

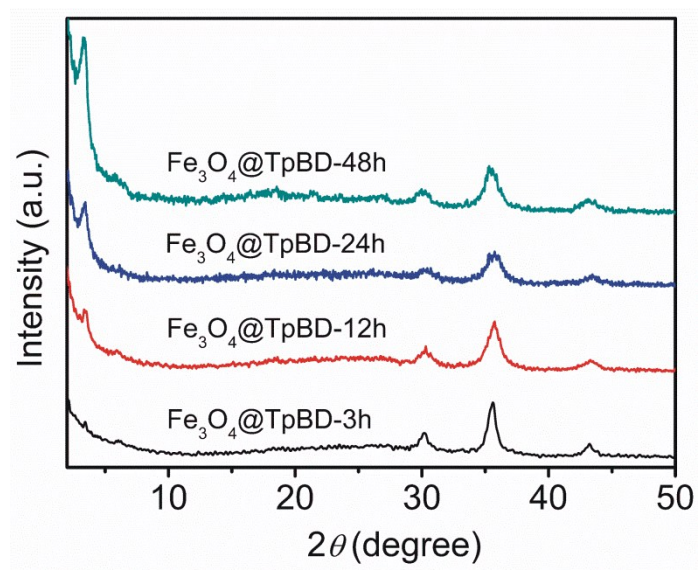


Figure S4. XRD patterns of TpBD prepared by a monomer-mediated in situ growth strategy for different reaction times.

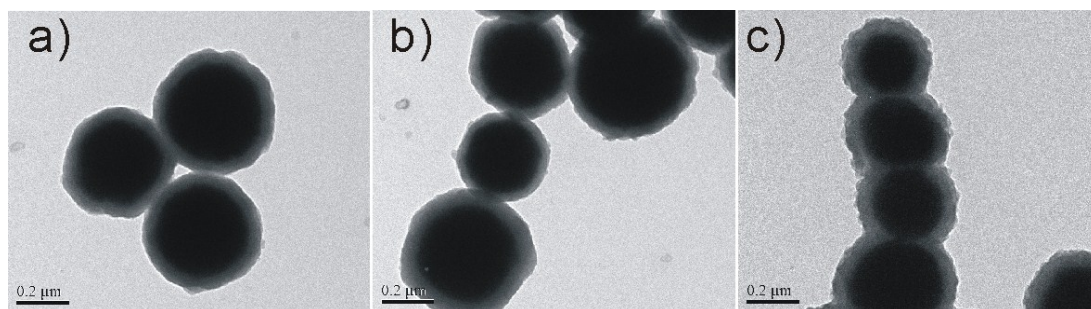


Figure S5. TEM images of the $\text{Fe}_3\text{O}_4@$ TpBD prepared with different reaction times: a) 3 h, b) 12 h, c) 24 h.

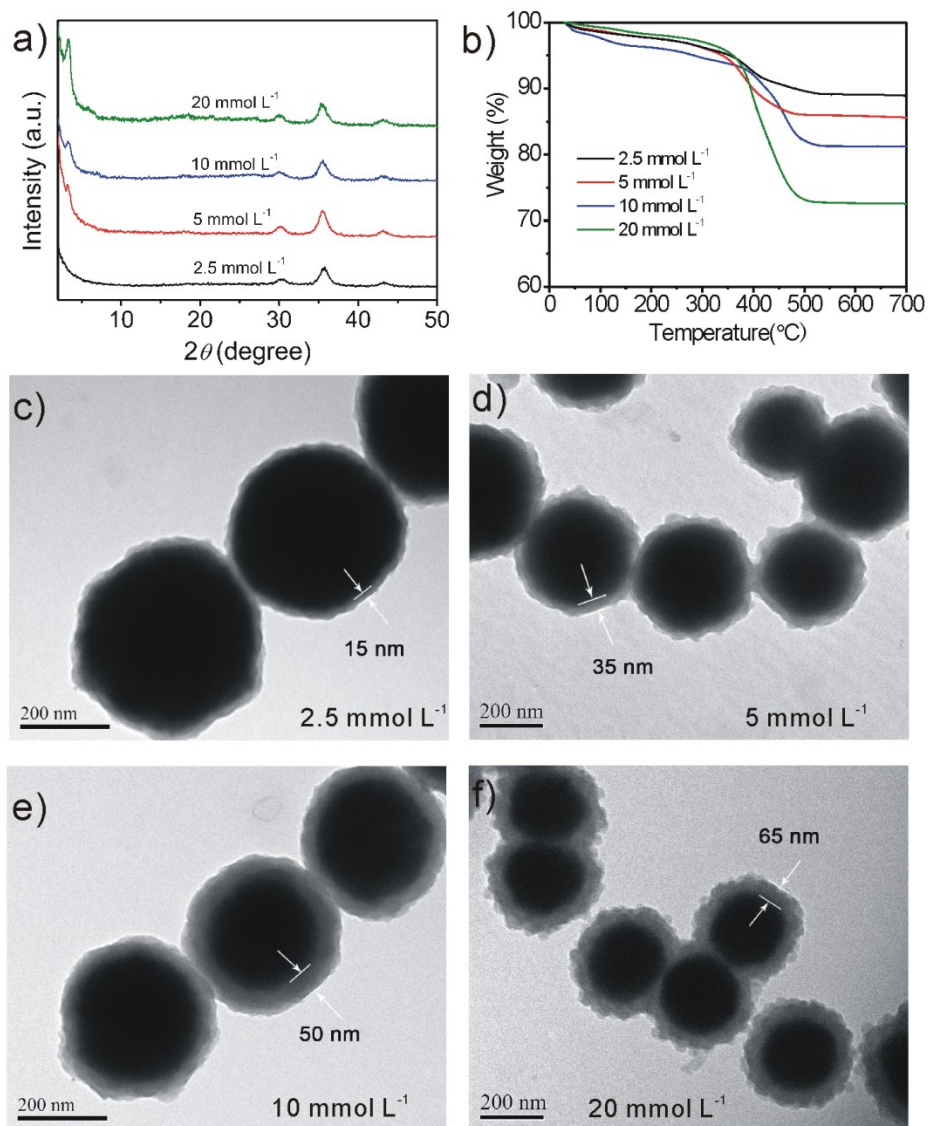


Figure S6. Effect of monomer concentration on Fe₃O₄@TpBD: a) XRD patterns; b) TGA curves; c-f) TEM images. TGA analysis shows a more weight loss at higher COF monomer concentrations.

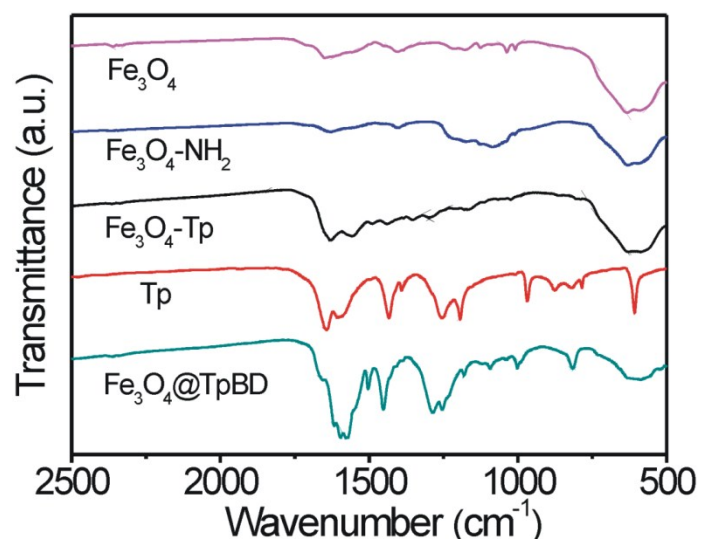


Figure S7. FT-IR spectra of Fe₃O₄, Fe₃O₄-NH₂, Fe₃O₄-Tp, Tp and Fe₃O₄@TpBD prepared by a monomer-mediated in situ growth strategy.

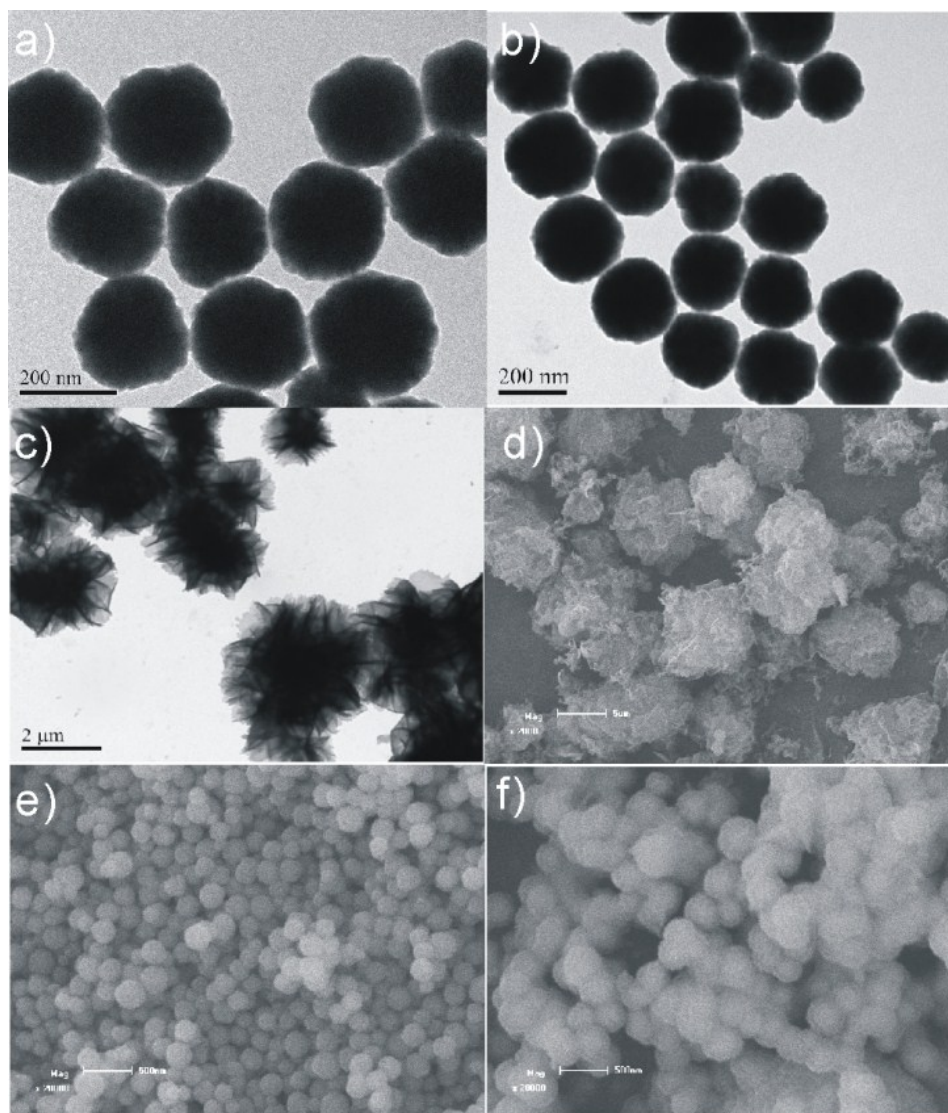


Figure S8. TEM images: a) $\text{Fe}_3\text{O}_4\text{-NH}_2$; b) $\text{Fe}_3\text{O}_4\text{-Tp}$; c) TpBD. SEM images; d) TpBD; e) Fe_3O_4 ; f) $\text{Fe}_3\text{O}_4\text{@TpBD}$ prepared by a monomer-mediated in situ growth strategy.

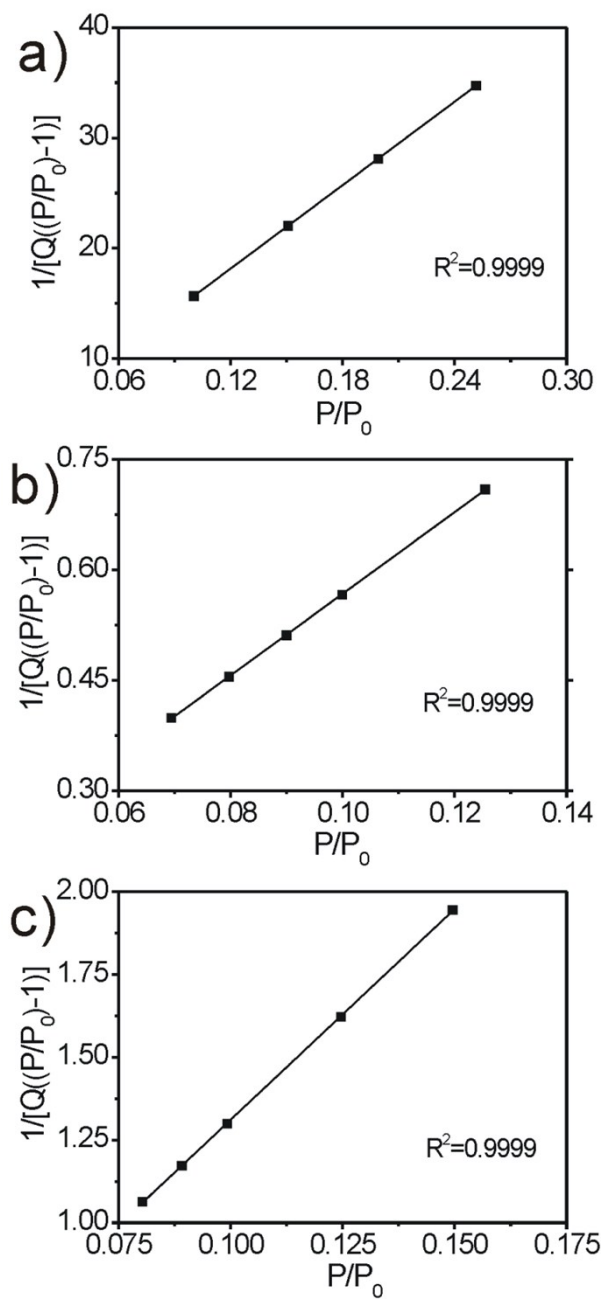


Figure S9. BET surface area plots derived from N₂ adsorption isotherms: a) Fe₃O₄; b) TpBD; c) Fe₃O₄@TpBD prepared by a monomer-mediated in situ growth strategy.

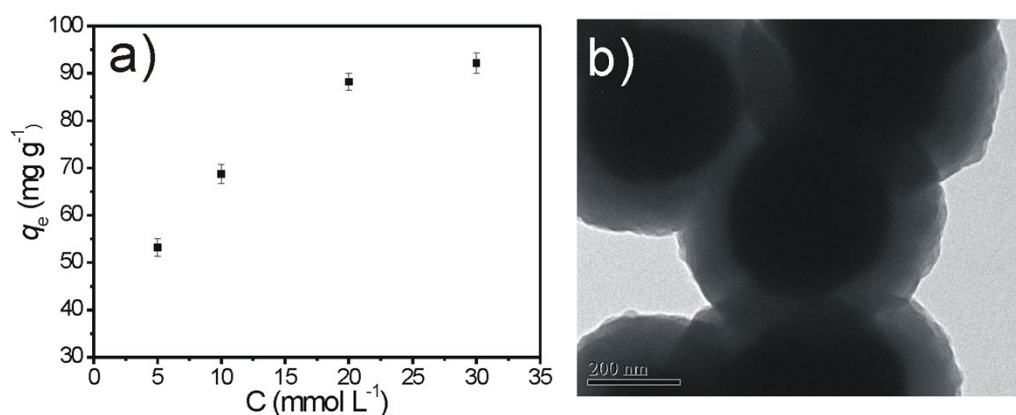


Figure S10. a) Adsorption capacities of Fe₃O₄@TpBD prepared with various COF monomer concentrations for the adsorption of BPA. b) TEM image of Fe₃O₄@TpBD prepared with the monomer concentration of 30 mmol L⁻¹. The adsorption ability increased slowly after the thickness of COF shell reached 65 nm (i.e. monomer concentration 20 mmol L⁻¹). Although higher monomer concentration led to thick COF shell, the composites became aggregated, resulting in weak magnetic property and much longer time for magnetic separation.

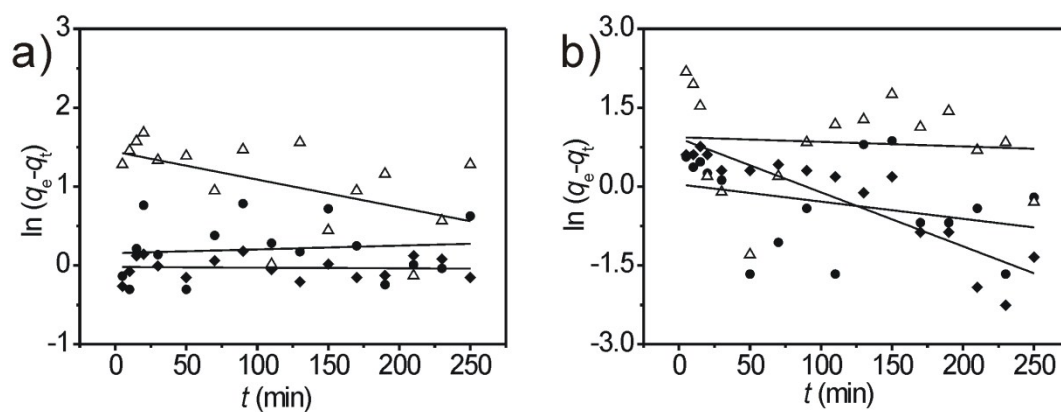


Figure S11. The plots of pseudo-first-order kinetics for the adsorption: a) BPA; b) BPAF with different initial concentrations (\blacklozenge : 50 mg L⁻¹, \bullet : 100 mg L⁻¹, Δ : 200 mg L⁻¹) at 298 K.

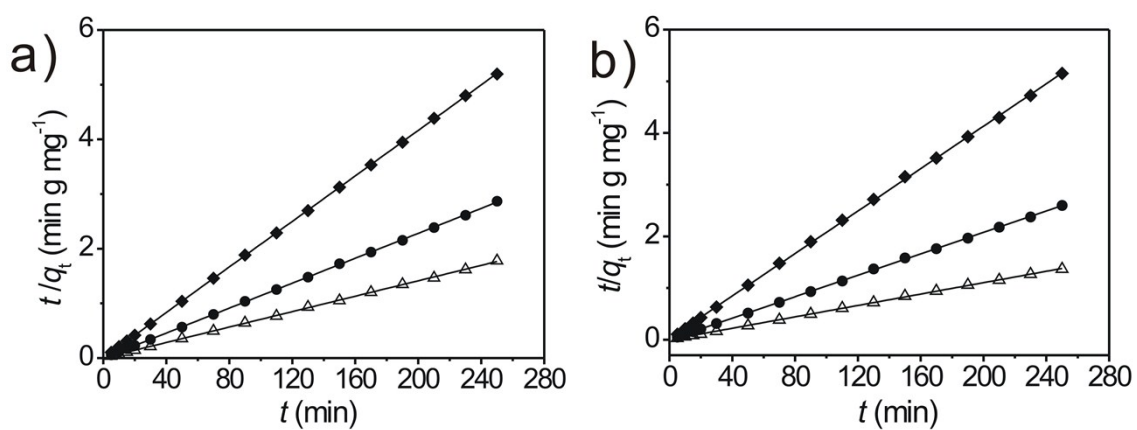


Figure S12. a) Plots of pseudo-second-order kinetics for BPA. b) Plots of pseudo-second-order kinetics for BPAF with different initial concentrations (\blacklozenge , 50 mg L⁻¹; \bullet , 100 mg L⁻¹; Δ , 200 mg L⁻¹) at 298 K.

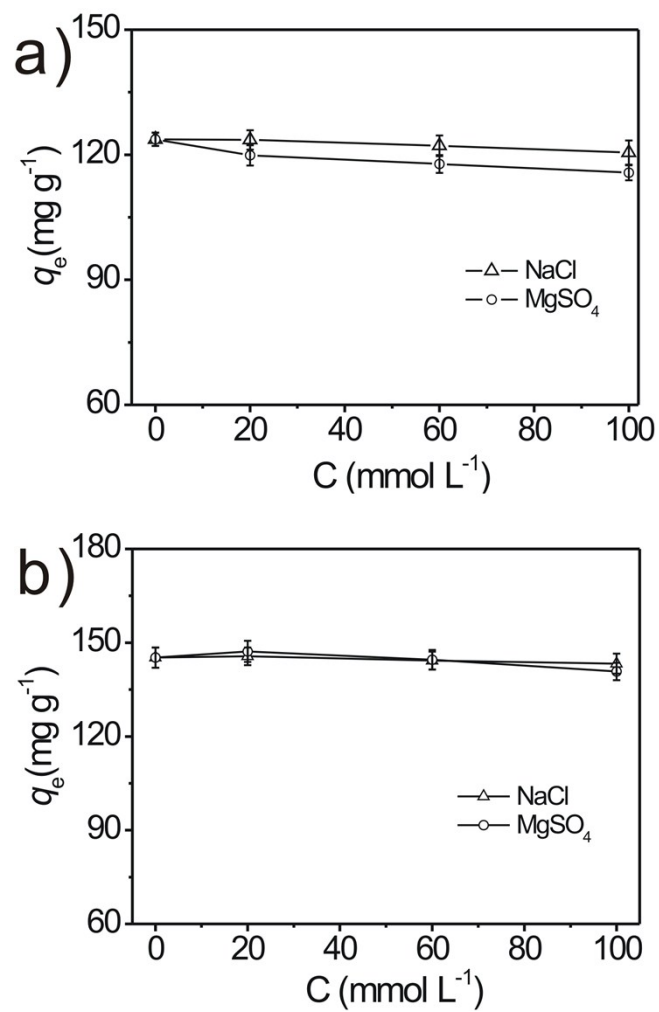


Figure S13. Effect of ionic strength on the adsorption on Fe₃O₄@TpBD at 298K: a) BPA; b) BPAF.

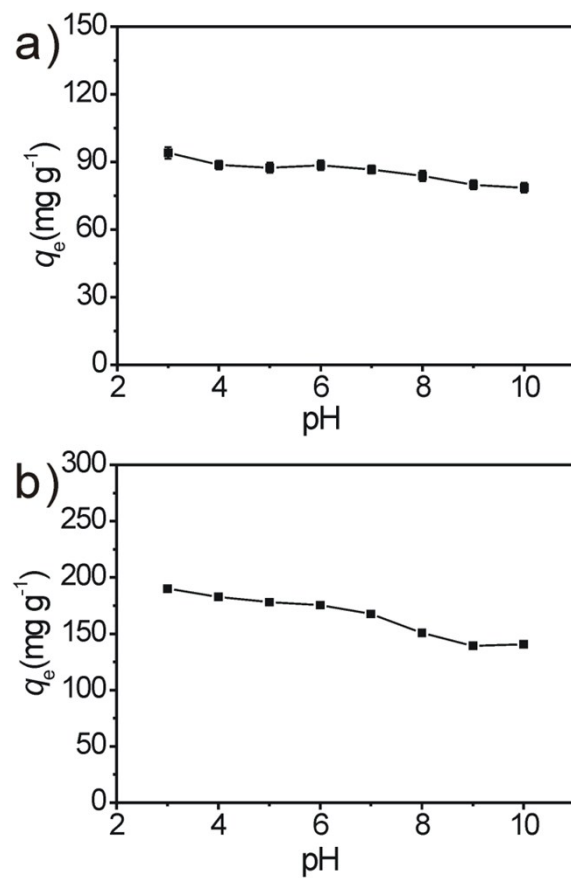


Figure S14. Effect of pH on the adsorption on Fe₃O₄@TpBD at 298K: a) BPA; b) BPAF.

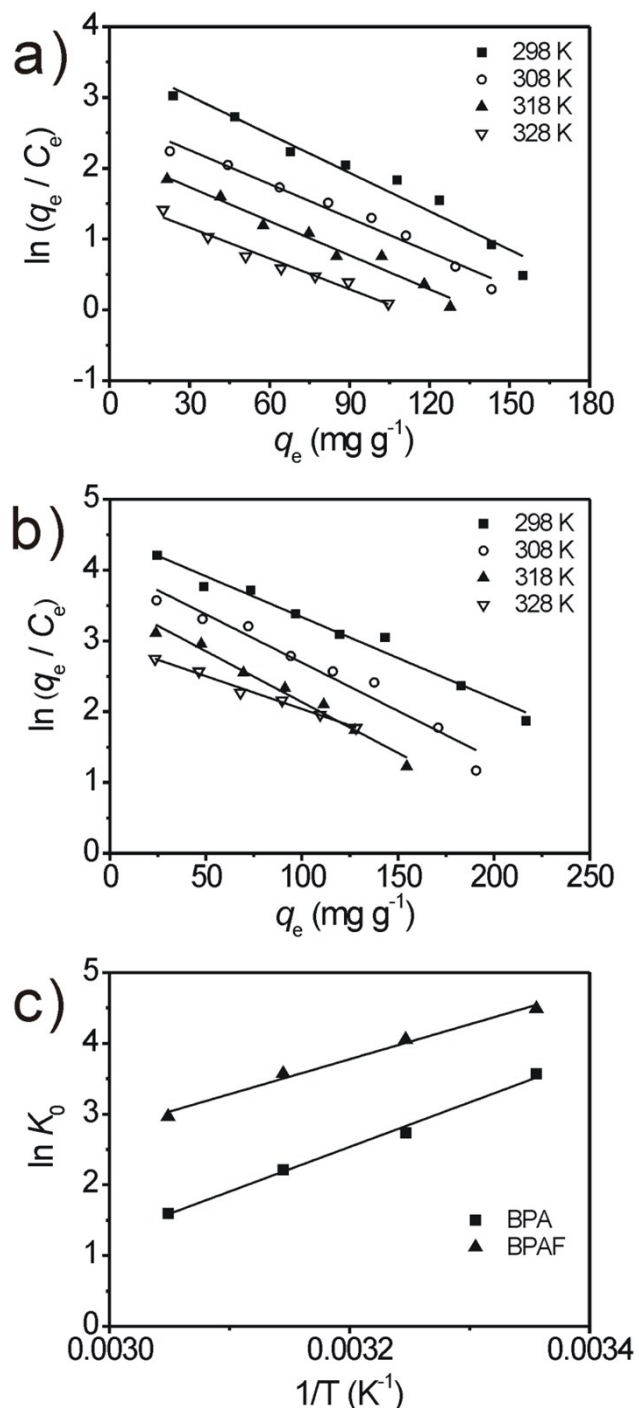


Figure S15. a) Plots of $\ln(C_s/C_e)$ vs. C_s at various temperatures for BPA. b) Plots of $\ln(C_s/C_e)$ vs. C_s at various temperatures for BPAF. c) Plots of $\ln K_0$ against $1/T$ for BPA and BPAF.

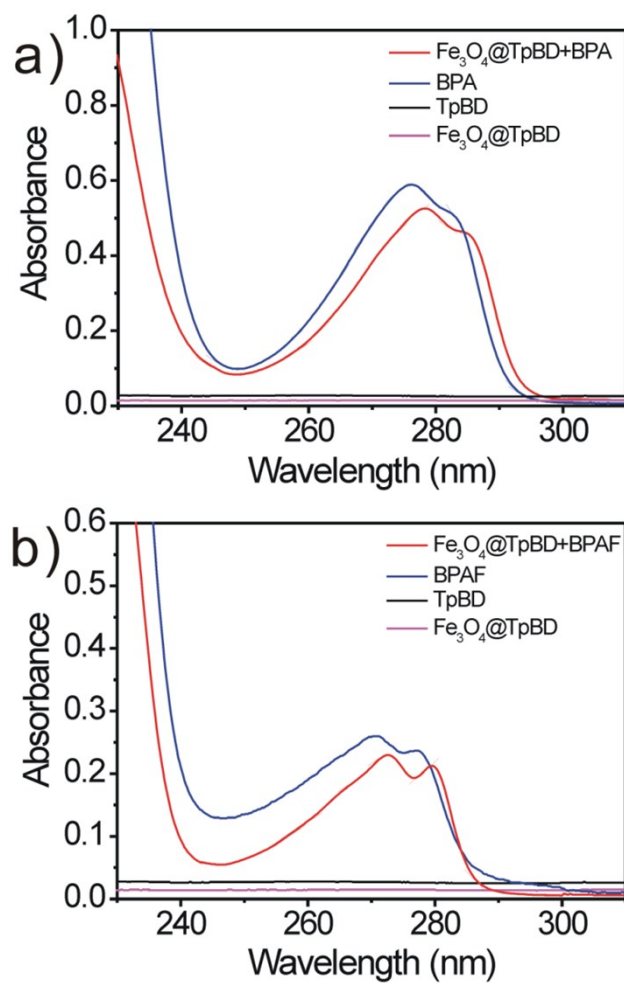


Figure S16. UV spectra: a) BPA; b) BPAF adsorbed on $\text{Fe}_3\text{O}_4@\text{TpBD}$ in aqueous suspension.

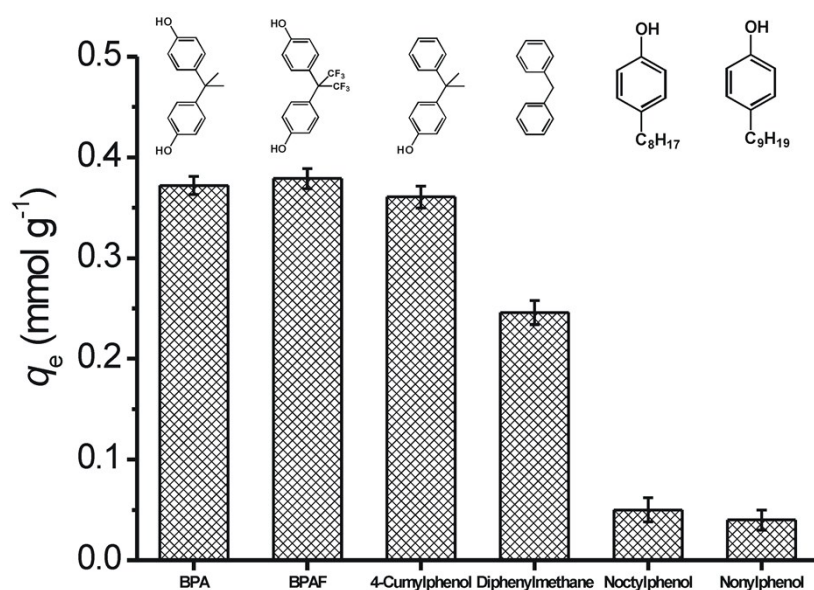


Figure S17. Adsorption on $\text{Fe}_3\text{O}_4@\text{TpBD}$ with initial concentration of 0.4 mmol L^{-1} .

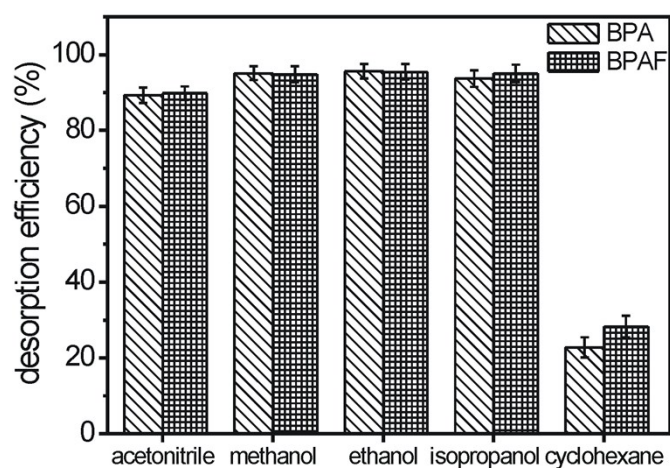


Figure S18. Effect of eluents on the desorption efficiency of BPA and BPAF.

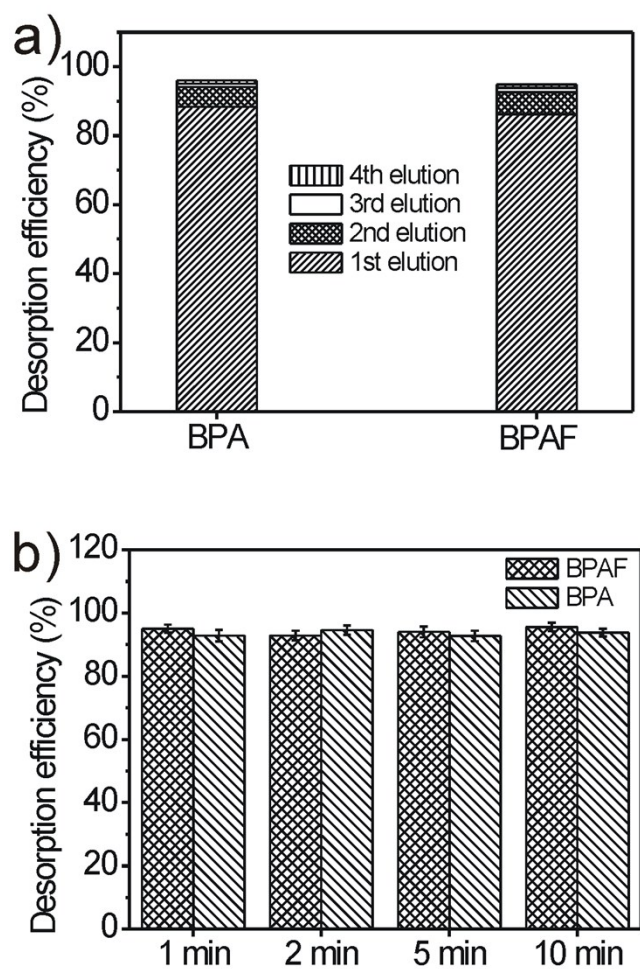


Figure S19. Effect of ethanol on desorption efficiency: a) Elution number. b) Elution time.

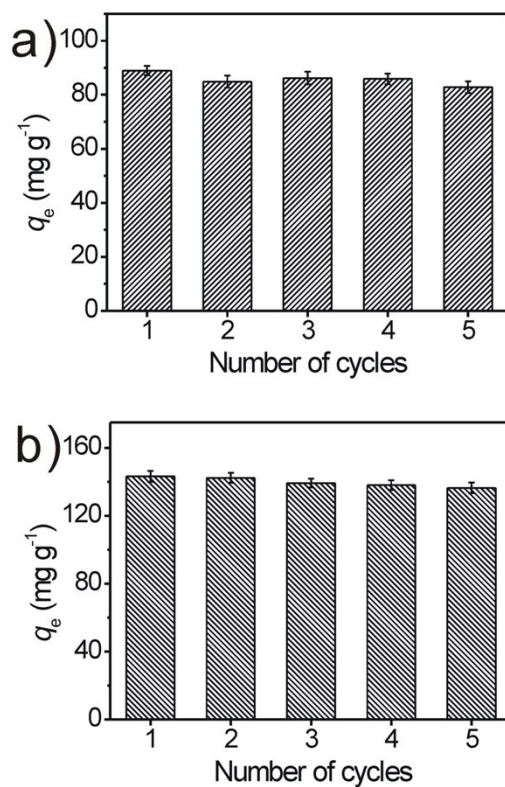


Figure S20. Recyclable adsorption on $\text{Fe}_3\text{O}_4@TpBD$: a) BPA; b) BPAF.

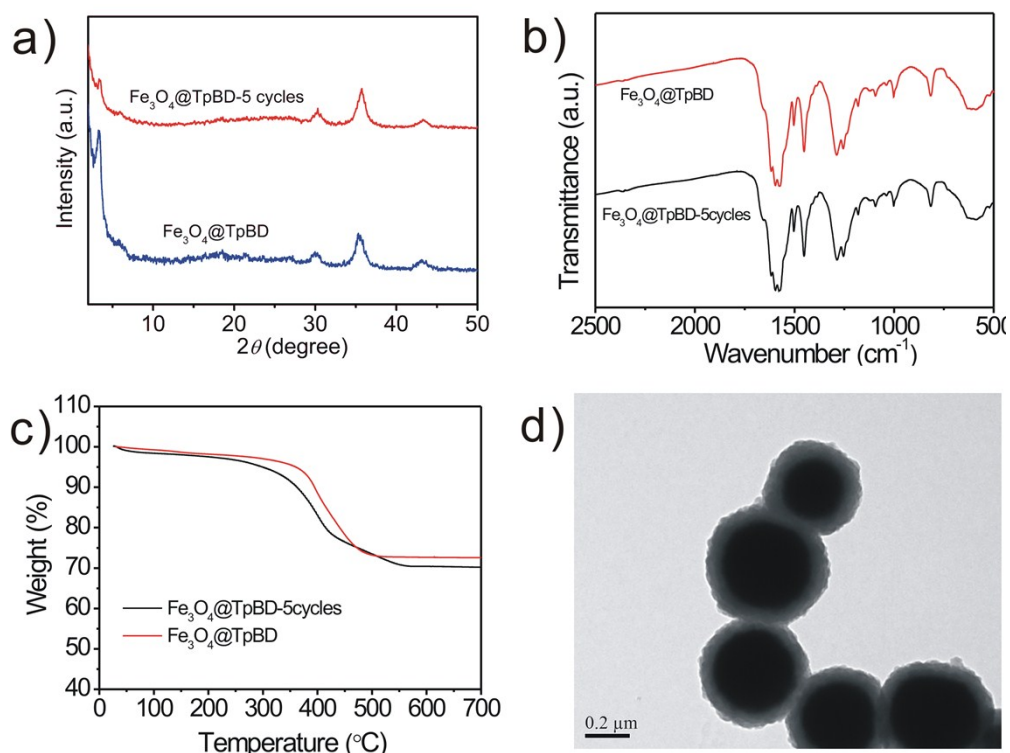


Figure S21. Characterization of $\text{Fe}_3\text{O}_4@TpBD$ after 5 times reuse: a) XRD patterns; b) FT-IR spectra; c) TGA curves; d) TEM images. The COF peak intensity at 3.3° in XRD pattern

decreases, but the peak position maintained unchanged and the IR spectra display no obvious change, indicating the maintenance of the corresponding functional group. The decrease in peak intensity of $\text{Fe}_3\text{O}_4@\text{TpBD}$ at 3.3° in XRD pattern indicates that repeated reuse may lead to partial loss of the COF shells.

Table S1. DLS and Zeta data of Fe₃O₄, Fe₃O₄-NH₂, TpBD and Fe₃O₄@TpBD.

	Hydrodynamic diameter (nm)	Zeta potential (mV)
Fe ₃ O ₄	297	-29.1
Fe ₃ O ₄ -NH ₂	311	-11.2
TpBD	4.6×10 ³	-23.3
Fe ₃ O ₄ @TpBD	450	-15.1

Table S2. Nitrogen adsorption-desorption data of Fe₃O₄, TpBD and Fe₃O₄@TpBD.

	BET surface area [m ² g ⁻¹]	Pore volume [cm ³ g ⁻¹]	Pore size [nm]
Fe ₃ O ₄	26.98	0.0545	30.5
TpBD	626.2	0.688	1.70
Fe ₃ O ₄ @TpBD	272.6	0.457	1.70

Table S3. Kinetic parameters for the adsorption of BPA and BPAF on Fe₃O₄@TpBD at 298 K.

	C ₀ ^{a)} [mg L ⁻¹]	q _e (exp) ^{b)} [mg g ⁻¹]	q _e (cal) [mg g ⁻¹]	k ₂ ^{c)} [g mg ⁻¹ min ⁻¹]	R ²
BPA	50	47.18 ± 1.12	48.03 ± 0.11	7.974 × 10 ⁻¹	0.9999
	100	88.17 ± 1.48	87.72 ± 0.40	2.382 × 10 ⁻¹	0.9999
	200	143.2 ± 2.9	141.6 ± 1.0	2.186 × 10 ⁻²	0.9998
BPAF	50	48.87 ± 1.44	48.71 ± 0.33	1.671 × 10 ⁻²	0.9998
	100	96.72 ± 1.88	96.43 ± 0.58	5.601 × 10 ⁻²	0.9999
	200	182.9 ± 3.5	181.5 ± 1.3	2.489 × 10 ⁻²	0.9998

a) Adsorption capacity at equilibrium

b) Initial concentrations of BPA and BPAF

c) Rate constant for pseudo-second-order adsorption

Table S4. Langmuir parameters for the adsorption of BPA and BPAF on Fe₃O₄@TpBD

	T [K]	q_0 [mg g ⁻¹]	b [L mg ⁻¹]	R^2
BPA	298	160.6 ± 5.4	0.135 ± 0.011	0.988
	308	154.6 ± 2.3	0.0676 ± 0.0028	0.997
	318	142.0 ± 4.7	0.0458 ± 0.0042	0.988
	328	134.0 ± 4.3	0.0289 ± 0.0024	0.989
BPAF	298	236.7 ± 8.3	0.249 ± 0.022	0.988
	308	198.1 ± 3.5	0.187 ± 0.010	0.996
	318	174.1 ± 3.1	0.133 ± 0.007	0.986
	328	164.9 ± 3.5	0.114 ± 0.007	0.994

Table S5. Comparison of the adsorption capacities of various adsorbents for BPA and BPAF

	Adsorbents	Equilibrium time [min]	Q_{\max}^b [mg g ⁻¹]	Ref.
BPA	Zeolite	10	111.1	1
	Activated carbon	NA ^{a)}	129.6	2
	Carbon nanotubes (CNTs)	30	61.0	3
	Magnetic reduced graphene oxides	600	48.7	4
	Magnetic molecularly imprinted polymers (MMIPs)	360	142.9	5
	Fe ₃ O ₄ @TpBD	5	160.6	This work
BPAF	Multi-walled carbon nanotube	4	88.89	6
	Chitosan-modified zeolite	1440	26.2	7
	Fe ₃ O ₄ @TpBD	5	236.7	This work

^{a)} Data not available.

b) Maximum sorption capacity at equilibrium.

Table S6. Thermodynamic parameters for the adsorption of BPA and BPAF on Fe₃O₄@TpBD

	<i>T</i> [K]	ln <i>K</i> ₀	Δ <i>G</i> [kJ mol ⁻¹]	Δ <i>H</i> [kJ mol ⁻¹]	Δ <i>S</i> [J mol ⁻¹ K ⁻¹]
BPA	298	3.567	-8.84	-52.32	-146.3
	308	2.737	-7.01		
	318	2.216	-5.86		
	328	1.598	-4.36		
BPAF	298	4.489	-11.1	-41.00	-99.82
	308	4.055	-10.4		
	318	3.571	-9.45		
	328	2.964	-8.09		

References:

- 1 W. T. Tsai, H. C. Hsu, T. Y. Su, K. Y. Lin, C. M. Lin, *J. Colloid. Interface Sci.* 2006, **299**, 513.
- 2 I. B. Toledo, M. A. Ferro-Garcia, J. Rivera-Utrilla, C. Moreno-Castilla, F. J. V. Fernandez, *Environ. Sci. Technol.* 2005, **39**, 6246.
- 3 C. Y. Kuo, *Desalination* 2009, **249**, 976.
- 4 Z. X. Jin, X. X. Wang, Y. B. Sun, Y. J. Ai, X. K. Wang, *Environ. Sci. Technol.* 2015, **49**, 9168.
- 5 W. L. Guo, W. Hu, J. M. Pan, H. C. Zhou, W. Guan, X. Wang, J. D. Dai, L. C. Xu, *Chem. Eng. J.* 2011, **171**, 603.
- 6 L. Zhang, J. N. Lv, T. C. Xu, L. J. Yang, X. Q. Jiang, Q. Li, *Sep. Purif. Technol.* 2013, **116**, 145.
- 7 S. Peng, K. Y. Hao, F. Han, Z. Tang, B. B. Niu, X. Zhang, Z. Wang, S. Hong, *Carbohydr. Polym.* 2015, **130**, 364.